Available online at www.sciencedirect.com
SCIENCE DIRECT
Sensors and Actuators A 130–131 (2006) 545–552
SENSORS AND ACTUATORS A PHYSICAL
www.elsevier.com/locate/sna

A lobster-sniffing inspired actuator for manipulation of micro-objects via controlling local fluid

Cheng-Hsiang Liu [a], Chia-Fang Chiang [a], Chieh Chang [a,b,1], Cheng-Hsien Liu [a,*]

[a] *Micro-Systems and Control Laboratory, Department of Power Mechanical Engineering, National Tsing-Hua University, Taiwan, ROC*
[b] *Mechanical Engineering Department, University of California at Berkeley, Berkeley, CA, USA*

Received 3 June 2005; received in revised form 9 September 2005; accepted 13 January 2006
Available online 20 February 2006

Abstract

Inspired by lobsters' sniffing behavior, an array of biomimic actuators are proposed for micro-particle manipulation in liquid. The engineering implementation of this lobster-tiny-hair-like capturing device is achieved by surface micromachining. These synthetic tiny-hair-like actuators are actuated via electrostatic force, and drive the micro-objects via disturbing the fluid field. The behind principle is to manipulate the Reynolds number of the surrounding fluid to achieve the function of micro-object manipulation. Numerical simulations are carried out to obtain the design criteria. Preliminary experimental results demonstrate the feasibility and functionality of our lobster-sniffing inspired actuator via the micro-object manipulation in liquid environment.
© 2006 Published by Elsevier B.V.

Keywords: Biomimic MEMS; Electrostatic actuator; Manipulation; Reynolds number

1. Introduction

Many applications in microbiology, biotechnology and clinical medicine require that individual cells can be identified as well as manipulated. Recent advances on the micro-electro-mechanical systems (MEMS) research are helping to offer satisfactory micro-bio-object platforms to further investigate the interactions between micro-objects like beads, proteins and cells [1]. Numerous manipulating techniques have been proposed over the past two decades such as microgripper [2,3], pneumatic microcage [4], and conjugated polymer actuator [5]. Most of these techniques take advantage of the clamping mechanism to achieve the grabbing function via direct contact. Moreover, the manipulating techniques via field variations have also been proposed and further studied lately. Optical tweezers, for example, utilize the force generated by the momentum transfer of refraction light to trap the targeted micro-object. Besides, arrays of these tweezers can be used to manipulate and direct objects in microfluidic systems [6]. Dielectrophoretic (DEP) particle traps have been widely studied to date. Such traps operate through the interaction of induced polarization charge with non-uniform electric fields and can induce trapping at either electrode edges (positive DEP) or electric field intensity minima (negative DEP) [7]. The capability and functionality of capturing live cells using these two methods has been demonstrated. Nevertheless, the equipment set-up of optical tweezers is pretty large and expensive while the practical applications for the manipulation of individual cells by DEP are still challenging. In this paper, we propose a novel actuator for the manipulation of micro-objects based on the Reynolds number manipulation of local surrounding fluid via MEMS technique.

2. Operating principle

The rich variety of mechanisms employed by swimming organisms has long been an inspiration for engineers and scientists. In nature, lobsters sniff for finding food, a suitable mate or to avoid predators by flicking their antennules (i.e. the second pair of antennae on the head of a crustacean) to capture fine patterns of odor molecules from the surrounding fluid. Lobsters' sniffing process could be classified into two stages. In the first stage, they change local fluid field by flicking their antennules with different velocities to bring odor molecules closer. Then,

* Corresponding author.
E-mail address: liuch@pme.nthu.edu.tw (Cheng-Hsien Liu).
[1] Mr. Chang has moved to UC Berkeley for his Ph.D. study since autumn 2005.

0924-4247/$ – see front matter © 2006 Published by Elsevier B.V.
doi:10.1016/j.sna.2006.01.026

in the second stage, these molecules get in contact with their chemosensory aesthetasc hairs to smell [8]. The way how lobsters bring targeted particles closer could be explained by using the concept of boundary layer and Reynolds number which has been studied by Koehl et al. [9]. The Reynolds number, denoted as Re, is mathematically represented as $Re = ul/v$, where u is the relative velocity, l is the characteristic length and v is the kinematic viscosity.

When a fluid moves relative to a solid body, the layer of fluid in contact with the surface of the body does not slip with respect to that surface. Hence, a velocity gradient, i.e. boundary layer, develops in the fluid between the surface and the freestream flow. The faster the relative velocity is (higher Re), the thinner the boundary layer is. On the contrary, the slower the relative velocity is (lower Re), the thicker the boundary layer is. In behalf of imitating the way lobsters control local fluid, we develop a biomimic MEMS actuator to realize micro-objects manipulation in liquid environment.

3. Device description

Fig. 1 shows SEM pictures of electrostatically actuated finger sets in the array arrangement. The MEMS fingers composed of bimorph beams curl up after the XeF_2 release process due to the mismatch of thermal expansion coefficients between aluminum layer and chromium layer. When there is a relative motion between fingers and their surrounding fluid, a boundary layer is formed around the fingers. First, the fingers are electrically driven in order to move downward by applying voltage on the bottom electrodes. Then the fingers move upward slowly by releasing the applied voltage. As illustrated in Fig. 2, during the fast downstroke, the finger sets act as a filter since the boundary layer is thin enough to allow the fluid to penetrate through the fingers' spacing. While fingers return to their initial position slowly, i.e. slow upstroke, the finger sets could be considered as a paddle because thick boundary layers fill up the gaps between

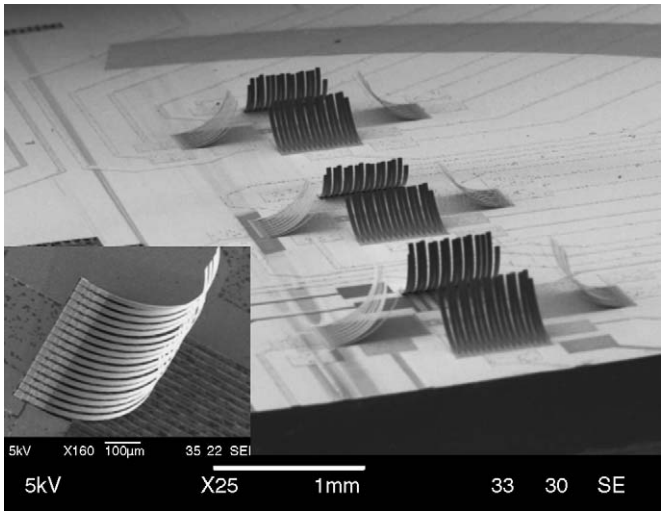

Fig. 1. SEM pictures of lobster-sniffing inspired electrostatic-actuated MEMS actuator in an array arrangement, showing only three units in this figure. The MEMS finger is 300 μm in length, 250 μm in height, 20 μm in width, 0.8 μm in thickness and 10 μm in the gap spacing.

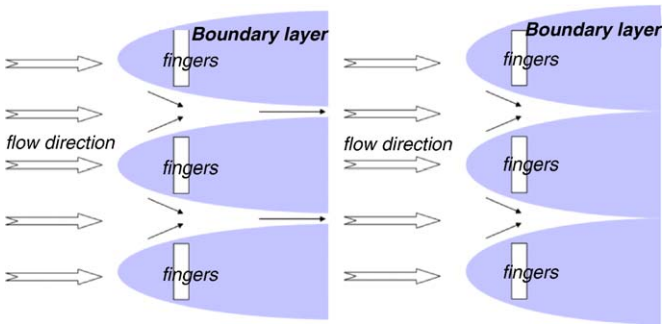

Fig. 2. Schematic illustration of the two operation modes with different fluid relative velocity. The left is the filter mode (fast velocity); the right is the paddle mode (slow velocity).

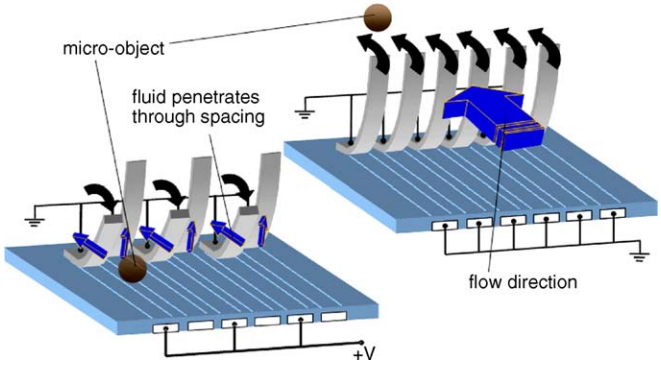

Fig. 3. Voltage control strategy for the biomimic actuator: odd and even fingers are drawn down separately (filter mode); all fingers curl up simultaneously (paddle mode).

each finger. For the paddle mode of our actuator finger sets, the return motion generates a drag force to bring the targeted particles closer to the fingers. The bottom electrode is connected to a high potential terminal while the finger sets are electrically grounded. An insulation layer is fabricated above the bottom electrode to prevent it from suffering short circuit effect. When the finger sets are actuated continuously, the particle could move toward a specific direction based on our temporal and spatial voltage control. Fig. 3 illustrates our voltage control strategy to achieve micro-object manipulation in liquid environment. Odd and even fingers are driven downward separately to enhance the filter effect and return to their initial position together for giving rise to a larger drag force. Hence, our lobster-sniffing inspired actuators could be operated in these two modes for achieving the function of particle manipulation.

4. Fabrication

The micro-fabrication of the lobster-sniffing inspired actuator is realized using surface micromachining technique. On the standard p-type ⟨1 0 0⟩ silicon wafer, thermal silicon dioxide is grown first to form an electric insulation layer. This is followed by depositing poly-silicon with phosphorous dopant which is patterned, then, to serve as bottom electrodes and wires as shown in Fig. 4(a). Next, the PECVD silicon dioxide is conformally deposited to serve as the second insulation layer to prevent the possible short circuit effect and bubble formation

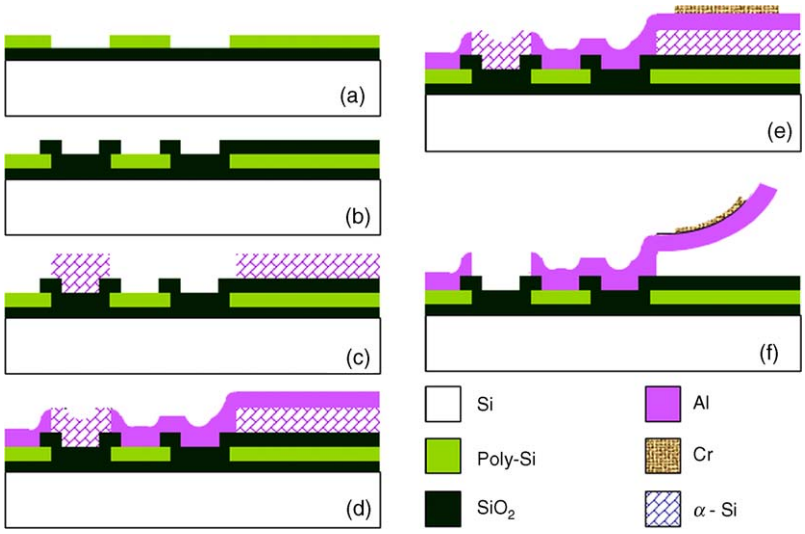

Fig. 4. Fabrication process of the lobster-sniffing inspired actuator.

during operation in liquid environment as shown in Fig. 4(b). The amorphous silicon deposited by PECVD is chosen to be the sacrificial layer and patterned by the RIE process to define anchor areas as illustrated in Fig. 4(c). The aluminum/chromium layer is then deposited on amorphous silicon for the main structure of actuation finger sets as shown in Fig. 4(d) and (e). The bimetal structure of the biomimic actuator mentioned above is fabricated using the lift-off process to define the aluminum/chromium layer in sequence. Finally, as shown in Fig. 4(f), all exposed amorphous silicon is removed by gas etchant, XeF_2, to release actuator and the fingers curl up due to residual stress.

5. Theoretical analyses and simulations

In our design, residual stress is crucial to our biomimic actuator, which greatly influences the shape and the height of the actuator. The curl angle of our MEMS fingers could be expressed with the parameter of curvature radius ρ. Judy et al. [10] proposed an equation relating the curvature radius ρ to the film thickness, h, the Young's Modulus, E, and the residual stress, σ, in the thin film, as shown in Eq. (1).

$$\rho = \frac{E_2 h(3m + (k/n(1+n)^2))}{6(m\sigma_2 - \sigma_1)} \quad (1)$$

where $k = 1 + 4mn + 6mn^2 + 4mn^3 + m^2n^4$, $h = h_1 + h_2$, $m = E_1/E_2$ and $n = h_1/h_2$. In our case, the bottom layer is set to be aluminum (subscript 1) and the upper layer is set to be chromium (subscript 2). The values of E_1 and E_2 are 70 and 140 GPa, respectively [11,12]. The values of σ_1 and σ_2, which depend on the fabrication process, are characterized via the thin film stress measurements of Tencor FLX-2320. The characterized residual stress values give the $(m\sigma_2 - \sigma_1)$ value of 1.0 GPa for our device. With the other design parameter, the thickness ratio of the bimorph layers, the radius of curvature can thus be obtained via Eq. (1). With the radius of curvature known, the end deflection of the bimetallic layer can be calculated from trigonometry.

According to the above theoretical derivation and experimental measurement data, Fig. 5 shows a family of curves for the curvature radius of our bimorph actuator fingers based on different designs. For fixed aluminum thickness (i.e. h_1 is constant), the radius of curvature decreases with the chromium thickness. The slope is sharp when the chromium thickness is within about 200 Å. These sharp slopes also imply the large variation on the curvature radius of our bimorph actuator fingers due to small micromachining uncertainty/variation. Furthermore, to achieve a small radius of curvature for curling up the actuator fingers, the thin aluminum layer is required. The thin thickness on the bimorph actuator fingers also refers to a low stiffness. The stiffness is an important parameter which greatly influences the required applied voltage on the bottom electrodes and the resonant frequency of our actuator fingers. The larger the stiffness, the larger the applied voltage is required. All of these are taken into account for the design of our MEMS actuator fingers.

A quasi-static analysis based on Rayleigh–Ritz method as well as small deflection theory is employed to investigate the phenomenon of pull-in voltage [13]. In this derivation, several approximations are assumed as the neglect of fringing field effect, which is commonly seen in the electrostatic application,

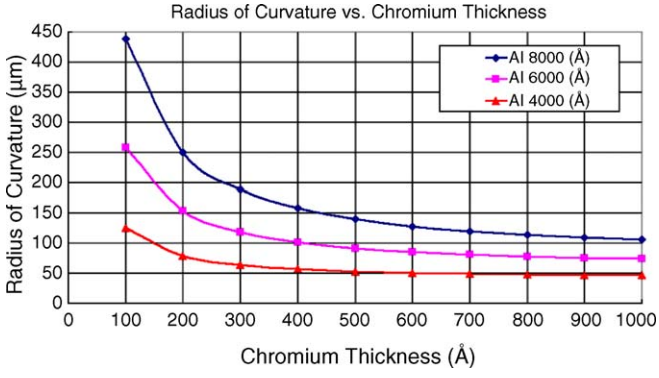

Fig. 5. Radius of curvature vs. chromium thickness at three fixed aluminum thickness values.

and the coupling effect resulted from the nearby fingers. From energy perspective, when a dc voltage is applied on the bottom electrode of our device, the total potential energy, denoted by π, equals to the sum of strain energy of bending, U_b, and the electrostatic potential energy, V_e, which can be expressed as [14]

$$\pi = U_b + V_e = \frac{EI}{2}\int_0^L \left(\frac{d^2W(x)}{dx^2}\right)^2 dx - \frac{1}{2}\int_0^L \frac{\varepsilon_0 b V^2}{g/\varepsilon_1 + y(x)/\varepsilon_2}\,dx \quad (2)$$

where EI is the bending stiffness of the finger; $W(x) = s(x) - y(x)$ is the static deflection; $s(x)$ is the original shape of the curled finger as a function of position x; $y(x)$ is the deflected shape of the curled finger as a function of position x; ε_0, ε_1, ε_2 are the dielectric constants of free space, of insulation layer, of operating environment, respectively; b is the finger width; g is the thickness of the insulation layer; and V is the driving voltage. These parameters as well as the aluminum layer thickness t are as illustrated in Fig. 6. With rearrangement and simplification, Eq. (2) can be expressed as the following equation, where c is a constant to be determined.

$$\pi = 72EIc^2\int_0^L (x-L)^4\,dx - \frac{1}{2}\varepsilon_0\varepsilon_1\varepsilon_2 WV^2\int_0^L \frac{1}{\varepsilon_2 g + \varepsilon_1 y(x)}\,dx \quad (3)$$

The pull-in voltage of the actuator fingers, V_{PI}, which is the critical value of the driving voltage V, could be obtained by finding the minimum potential energy via the principle of virtual work. The pull-in voltage means the critical applied potential that makes the transition for the actuator fingers from the stable equilibrium to the unstable status. The pulling voltage of the actuator fingers, V_{PI}, could be solved by setting the first and the second variation of the total potential energy with respect to the constant c to be zero as shown in Eqs. (4) and (5).

$$\frac{\partial\pi}{\partial c} = 144EIc\int_0^L (x-L)^4\,dx + \frac{1}{2}\varepsilon_0\varepsilon_1^2\varepsilon_2 WV^2\int_0^L \frac{x^4 - 4Lx^3 + 6L^2x^2}{[\varepsilon_2 g + \varepsilon_1 y(x)]^2}\,dx = 0 \quad (4)$$

$$\frac{\partial^2\pi}{\partial c^2} = 144EI\int_0^L (x-L)^4\,dx - \varepsilon_0\varepsilon_1^3\varepsilon_2 WV^2\int_0^L \frac{(x^4 - 4Lx^3 + 6L^2x^2)^2}{[\varepsilon_2 g + \varepsilon_1 y(x)]^3}\,dx = 0 \quad (5)$$

By solving these two partial differential equations simultaneously, the pull-in voltage of the actuator finger, V_{PI}, and the critical value c_{PI} for the constant c at pull-in condition can be calculated as follows.

$$V_{PI}^2 = \frac{12t^3EL^5}{5\varepsilon_0\varepsilon_1^3\varepsilon_2}\frac{1}{\int_0^L (x^4 - 4Lx^3 + 6L^2x^2)^2/[\varepsilon_2 g + \varepsilon_1 y(x)]^3 dx} \quad (6)$$

$$c_{PI} = -\frac{1}{2\varepsilon_1}\frac{\int_0^L x^4 - 4Lx^3 + 6L^2x^2/[\varepsilon_2 g + \varepsilon_1 y(x)]^2 dx}{\int_0^L (x^4 - 4Lx^3 + 6L^2x^2)^2/[\varepsilon_2 g + \varepsilon_1 y(x)]^3 dx} \quad (7)$$

From Eqs. (6) and (7), they show that the finger width, b, does not affect the pull-in voltage. Besides, finger bending stiffness, EI, and finger thickness, t, do not contribute to the maximum displacement before pull-in since c_{PI} is independent of these parameters. In accordance with the theoretical analyses, the width of the finger has little effect on the pull-in voltage. It is also observed that actuating fingers with longer length or thinner thickness have smaller mechanical stiffness to compete against electrostatic force, that is to say, these fingers can be driven with lower applied voltage. Fig. 7 shows the tip displacement of the actuator finger versus the applied voltage for both simulation and experimental results. These results are characterized by using WYKO profiling system. WYKO surface profiler uses interfermetric principle and produces interference fringes by combining the light reflected from the sample with the light reflected from a reference mirror for the surface profile identification. During our tip-displacement experiments, the original

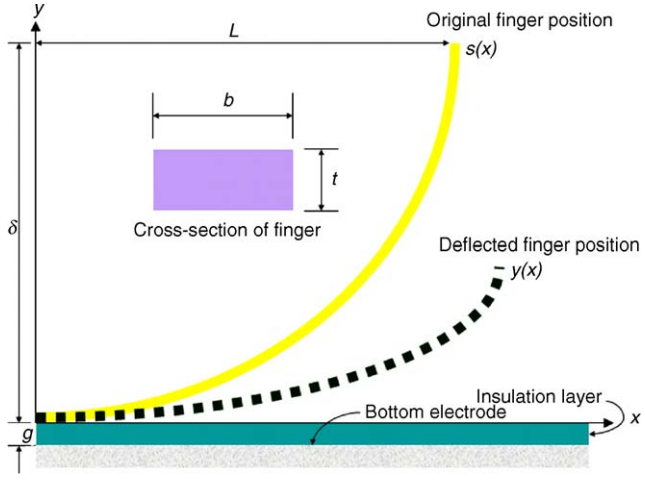

Fig. 6. Schematic illustration of curled finger (side view) with the definition of the dimensions and parameters required for the theoretical analyses.

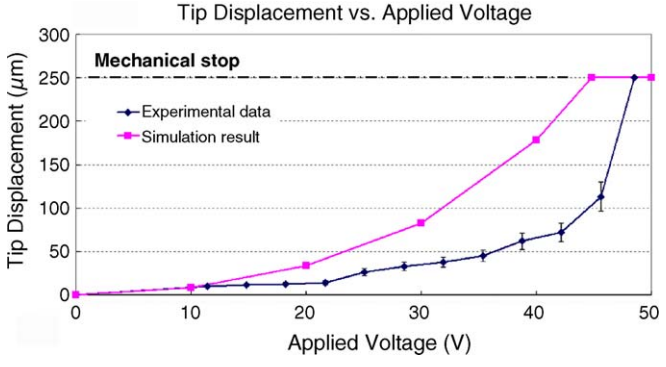

Fig. 7. Tip displacement of the biomimic actuator fingers versus applied voltage.

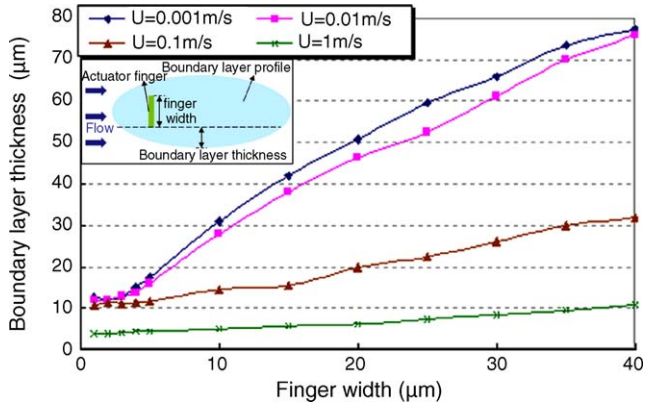

Fig. 8. The boundary layer thickness vs. the width of the biomimic actuator finger for different actuating velocities ranging from 0.001 to 1 ms^{-1}.

position of the actuator fingers is characterized first. Then, the different dc voltages are applied on the actuator fingers for the measurements of the steady-state tip displacements under different applied potentials. The difference between simulation and experimental results mainly results from the parameter variation owing to fabrication uncertainty constraint.

In regard to the fluid field analysis, the commercial software package developed by CFDRC is utilized to simulate this complicated problem. Fig. 8 shows the simulation results for the boundary layer thickness versus the finger width with the different actuating velocities ranging from 0.001 to 1 ms^{-1}. From these simulation results, the higher relative velocity between the finger and its surrounding fluid gives rise to thinner boundary layer. On the contrary, lower relative velocity leads to thicker boundary layer. As shown in Fig. 8, the actuator finger width is of little significance on the boundary layer thickness at high relative velocity. However, the influence of the finger width with respect to the boundary layer thickness turns out to be much more apparent with the decrease of the relative velocity. These results assist us to optimize the parameters design of our biomimic actuator fingers to minimize the effects of micro-fabrication variations and operation uncertainties. The simulation results of fluid flowing through the different actuator finger sets with different relative flow velocities are shown in Fig. 9. Fig. 9(a) shows the filter mode (large Reynolds number) in which the fluid penetrates through the fingers' spacing. Fig. 9(b) shows the paddle mode (small Reynolds number) in which the boundary layer is thick enough to stem the fluid flowing through the fingers' spacing. These simulation results represent the feasibility of the voltage control strategy to operate odd and even fingers separately or simultaneously to mimic the functions which lobsters use to find food and a suitable mate via capturing odor molecules from the surrounding fluid.

The results of modal analysis using CoventorWare, a commercial MEMS design/simulation tool developed by Coventor, assist in modifying our design to find out the appropriate vibration mode for our device to result in appropriate operation. The thicker the finger is, the less coupling effect among different modes will be [12]. As a result, higher energy is required to excite other higher vibration modes for the fact that thicker finger results in stronger stiffness. Comparing to the aluminum

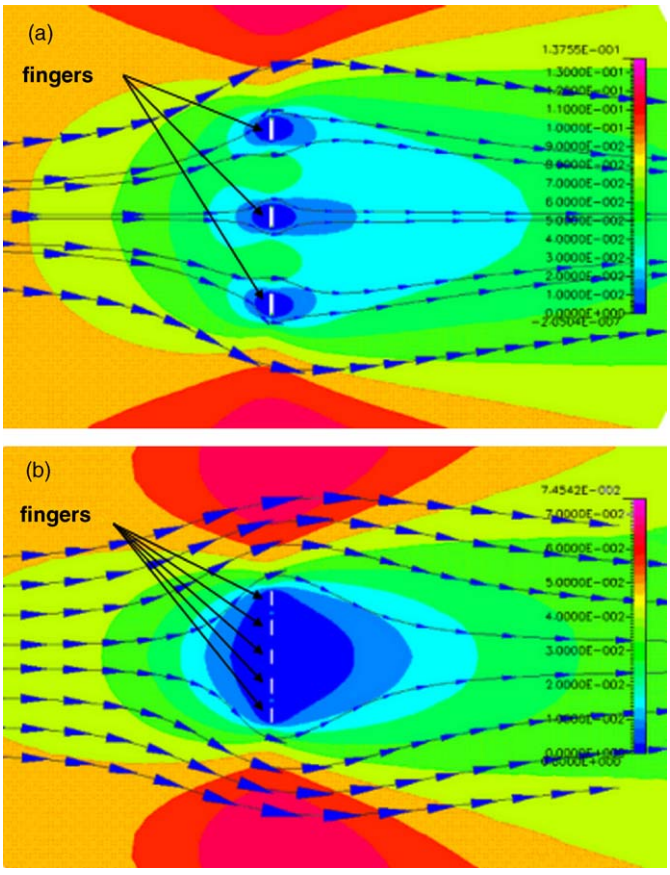

Fig. 9. Simulation results of fluid flowing through the actuator finger set. (a) The finger width, gap spacing, and relative flow velocity are set as 5 μm, 15 μm, and 1 ms^{-1}, respectively, in this filter mode simulation. (b) The finger width, gap spacing, and relative flow velocity are set as 5 μm, 5 μm, and 0.05 ms^{-1}, respectively, in this paddle mode simulation.

layer, chromium layer for our device is thin enough that the stiffness effect can be ignored in these analyses. The liquid damping effects are also neglected owing to simplicity in these modal analyses. Fig. 10 shows the simulation results of three different vibration modes performed by using the ConventorWare. The first vibration mode exhibits the up and down stroking behavior, which corresponds to the direction of pull-in phenomenon. The second vibration mode exhibits the left and right swinging behavior, whereas the third vibration mode exhibits the stretching and bending behavior. Nevertheless, the first vibration mode is desired for our actuators to be operated under and the higher vibration modes such as the second and the third modes are supposed to be minimized during the operation, because there is only single actuation electrode on the bottom substrate in our design. It is concluded that an increase of the actuator finger thickness could minimize the dynamic coupling effect of higher vibration modes while the actuator fingers are operated under the first vibration resonance. The resonant frequency of the first vibration mode, in our CoventorWare simulation results, is 834 Hz for the actuator fingers of 0.1 μm in total Cr/Al thickness. In our preliminary experimental tests, the actuator fingers with the total thickness of 0.1 μm/or even 0.2 μm are broken and hard to survive against the liquid surface tension at the begin-

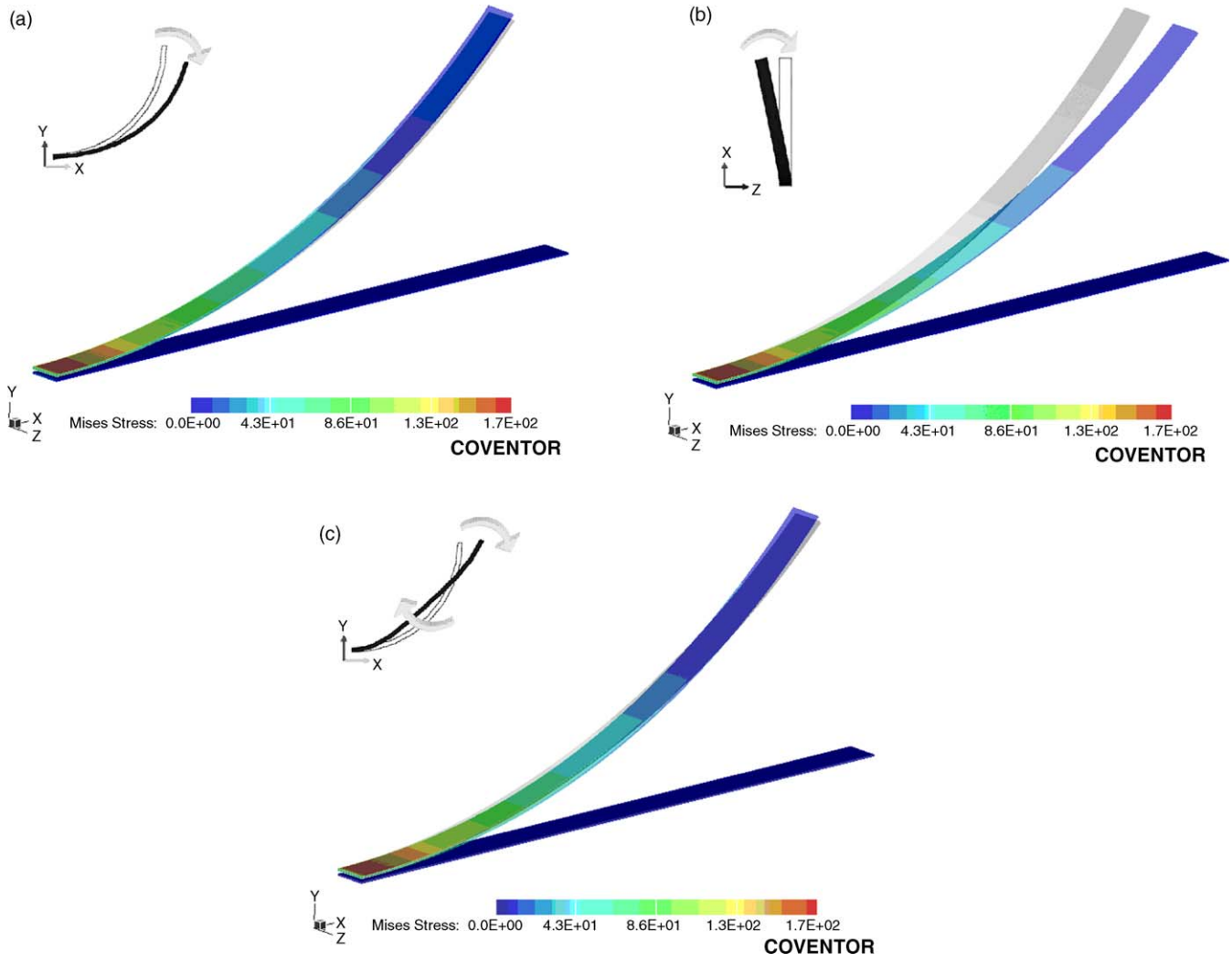

Fig. 10. Schematic illustration of three different vibration modes. (a) The up and down stroke mode; (b) the left and right swing mode; (c) the stretch and bend mode.

ning of liquid injection. Because the actuator fingers are aimed at being operated in the liquid environment, finger total thickness larger than 0.1 μm is designed in our device. As shown in Fig. 1, the devices with the actuator fingers of the total thickness of about 0.8 μm are utilized for all experimental characterization in this paper. As addressed above, however, larger finger thickness leads to higher actuating voltage, and this is a tradeoff needed to be consider thoroughly. Consequently, the primary goal is to design the actuator finger with a high vibration frequency to allow the actuator fingers to operate at a speed as high as possible in the fluid environment under the circumstances of low actuating voltage.

6. Experimental results

Polytech laser doppler vibrometer (LDV) is utilized to characterize the resonant frequencies of the actuator fingers for studying the dynamics of the curled actuator fingers. Fig. 11 shows the resonant frequencies measured in air where the first vibration mode appears at 5.2 kHz, the second vibration mode appears at 12.5 kHz and the third vibration mode appears at 20.3 kHz. It is expected that the resonant frequencies shift slightly to higher values while operating in liquid since the liquid environment contributes higher damping effect and more viscosity than the air environment.

We have tested our device both in air and liquid environment such as water, 3 M Fluorinert liquid (FC-40), and dimethyl sulfoxide (DMSO). The permittivity and specific gravity of Fluorinert are 1.89 and 1.85, respectively. Both Fluorinert and

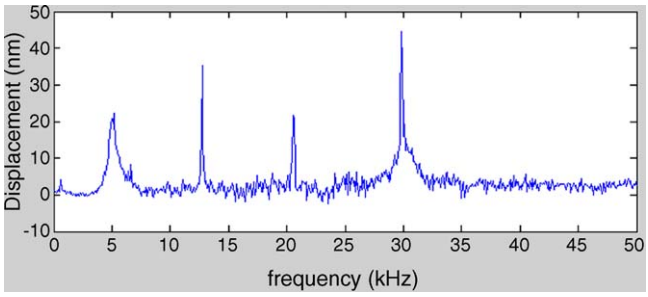

Fig. 11. The resonant frequency measurement using Polytec laser doppler vibrometer. The testing finger has 300 μm in length, 250 μm in height, 20 μm in width and 0.8 μm in thickness.

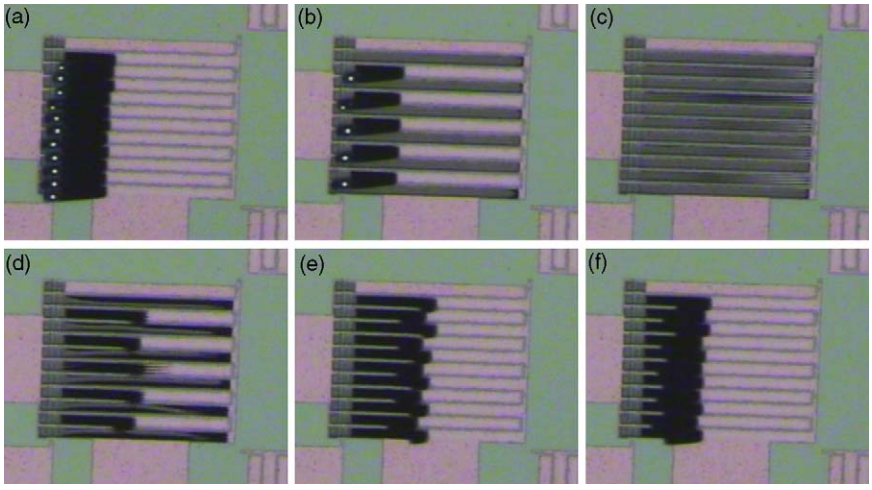

Fig. 12. Sequential frames captured from a video showing the process of the biomimic finger actuation with the applied voltage: (a)–(c) actuator fingers zip along the bottom electrode with odd and even fingers driven separately; (d)–(f) actuator fingers curl to their original position with odd and even fingers released separately.

DMSO have the characteristic of lower electrical conductivity than water, therefore, they are suitable solutions for our device to actuate in without the issue of thermal bubble formation for the concept-proof demonstration shown in this paper. When a dc voltage is applied on the bottom electrodes, the actuator fingers will deflect and zip along the bottom electrodes in accordance with the specific range of applied voltage. Generally, the actuator fingers start zipping along the bottom electrode at about 40–50 V and the pull-in phenomenon occurs at the voltage higher than 60–100 V. The capability of the finger actuation as well as the micro-particle manipulation in Fluorinert and water is observed in our preliminary experiments. As shown in Fig. 12, when the voltage is applied, the actuator fingers start zipping down and the pull-in occurs in a few milliseconds. When the applied voltage is removed, the actuator fingers slowly curl up and return to the original position.

In these prototypes, the operation range of applied voltage varies. These variations might result from the fabrication uncertainties such as the thickness variation of aluminum and chromium layers, and the non-uniformity of insulation layer. In our recent runs via the cleanroom facility available, even the PECVD silicon dioxide process ever results in about 40% thickness variation across a single wafer. Finger sets with thicker isolation layer lead to the higher pull-in voltage, while thinner isolation layers give rise to the lower pull-in voltage. In addition, due to the microfabrication uncertainties and parameter variations, the poor coverage and the uniformity of isolation layer give rise to the current leakage problem, which results in bubbles during actuation operation, especially for high-voltage operation. The voltage for electrolysis greatly lies on whether the bottom electrodes are sealed well by insulation layer.

7. Conclusion

A lobster-sniffing inspired actuator for micro-objects manipulation in liquid environment using electrostatic actuation is proposed in this paper. Structural analyses, electromechanical simulation and the model simulation which investigates the interaction between the biomimic actuator and their surrounding fluid are carried out to acquire design criteria. The feasibility and functionality of micro-object manipulation by varying local fluid field is experimentally observed. Since our device manipulates particles via controlling the fluid surrounding the targeted particles, it is a potential tool having non-contact and non-invasive advantages for the application of micro-manipulation in liquid environment. However, the electrolysis/thermal bubble issue must be overcome when this proposed approach is applied to practical bio-object manipulation in different conductive buffer solutions. In this paper, for concept-proof demonstration, both Fluorinert and DMSO are utilized. Currently, AC driving voltage with lower voltage amplitude is under study in our group to extend this application to practical bio-object manipulation in different conductive buffer solutions. Besides, different materials and actuation transducers are also worth to study to implement this learn-from-nature idea. With array formation integrated with image processing mechanism, massive parallel biological applications including micro-bio-object positioning, cell patterning and drug development will be the primary target for investigation in future research.

Acknowledgments

This research was supported partially by the Nanotechnology Research Program of University System of Taiwan, ROC. The authors acknowledge Professor Long Hsu, Professor Hwan-You Chang and Professor Hwei-Ling Peng for their brainstorm. The authors would like to thank Mr. Chin-Chen Tu for his microfabrication assists and constructive discussions. This research is inspired by the talk of UC Berkeley's Professor M.A.R. Koehl given at Stanford University in year 2000.

References

[1] J. Voldman, BioMEMS: building with cells, Nat. Mater. 2 (2003) 433–434.
[2] C.J. Kim, A.P. Pisano, R.S. Muller, Silicon-processed overhanging microgripper, J. Microelectromech. Syst. 1 (1992) 31–36.

[3] A.P. Lee, D.R. Ciarlo, P.A. Krulevitch, J. Trevino, M.A. Northrup, A practical microgripper by fine alignment, eutectic bonding and SMA actuation, in: Proceedings of the Int. Conf. on Solid-State Sensors and Actuators, Transducers'95, vol. 2, Stockholm, Sweden, June 25–29, 1995, pp. 368–371.
[4] J. Ok, M. Chu, C.J. Kim, Pneumatically driven microcage for micro-objects in biological liquid, in: Proceedings of the IEEE Intl. Conf. on Microelectromechanical Systems (MEMS)'99, Orlando, Florida, USA, January 17–21, 1999, pp. 459–463.
[5] E.W.H. Jager, E. Smela, O. Inganäs, Microfabricating conjugated polymer actuators, Science 290 (2000) 1540–1545.
[6] M. Ozkan, M. Wang, C. Ozkan, R. Flynn, S. Esener, Optical manipulation of objects and biological cells in microfluidic devices, Biomed. Microdevices 5 (1) (2003) 61–67.
[7] J. Voldman, R.A. Braff, M. Toner, M.L. Gray, M.A. Schmidt, Holding forces of single-particle dielectrophoretic traps, Biophys. J. 80 (2001) 531–541.
[8] C. Loudon, B.A. Best, M.A.R. Koehl, When does motion relative to neighboring surfaces alter the flow through arrays of hairs? J. Exp. Biol. 193 (1994) 233–254.
[9] M.A.R. Koehl, J.R. Koseff, J.P. Crimaldi, M.G. McCay, T. Cooper, M.B. Wiley, P.A. Moore, Lobster sniffing: antennule design and hydrodynamic filtering of information in an odor plume, Science 294 (2001) 1948–1951.
[10] M.W. Judy, Y.H. Cho, R.T. Howe, A.P. Pisano, Self-adjusting microstructures (SAMS), in: Proceedings of the IEEE MEMS Workshop '91, January 30–Feburary 2, 1991, Nara, Japan, pp. 51–56.
[11] The material, property database from ConventorWare.
[12] http://www.memsnetorg/material.
[13] C. Chang, C.F. Chiang, C.-H. Liu, C.-H. Liu, A lobster-sniffing-inspired method for micro-objects manipulation using electrostatic micro-actuators, J. Micromech. Microeng. 15 (2005) 812–821.
[14] R. Legtenberg, J. Gilbert, S.D. Senturia, M. Elwenspoek, Electrostatic curved electrode actuators, J. Microelectromech. Syst. 6 (1997) 257–265.

Biographies

Cheng-Hsiang Liu received the BS degree in power mechanical engineering from National Tsing-Hua University, Taiwan, ROC, in 2003. Currently, he is a graduate student and a member at Micro-Systems and Control Laboratory, Power Mechanical Engineering Department, National Tsing-Hua University. His research interests include microfabrication technologies, system control and signal processing.

Chia-Fang Chiang received the BS degrees in power mechanical engineering from National Tsing-Hua University, Taiwan, ROC, in 2003. Currently, she is a graduate student and a member at Micro-Systems and Control Laboratory, Power Mechanical Engineering Department, National Tsing-Hua University. Her research interests include system control engineering and MEMS for biomedical applications.

Chieh Chang received the BS and the MS degrees in power mechanical engineering from National Tsing-Hua University, Taiwan, ROC, in 2001 and 2003, respectively. Since October 2003, he has been in military service as a reserve officer. While at National Tsing-Hua University, he worked at Micro-Systems and Control Laboratory, focusing on the development of lobster antennules-like micro-actuators for the Manipulation of Biology Objects. In year 2005, he received the admission for PhD study at University of California at Berkeley. He will join Berkeley in autumn 2005 after his military service. His research interests include microfabrication technologies, system control, microfluidics and BioMEMS.

Cheng-Hsien Liu received the BS degree in power mechanical engineering from National Tsing-Hua University, Taiwan, ROC, in 1987, the MS degree in mechanical engineering from Lehigh University, Bethlehem, PA, in 1992, the MS degree in electrical engineering and the PhD degree in mechanical engineering from Stanford University, CA, in 1995 and 2000, respectively. Since autumn 2000, he has been with National Tsing-Hua University, Taiwan, ROC, as an assistant professor in Power Mechanical Engineering Department. In 1999–2000, he worked as a senior Electrical Engineer at Halo Data Devices Inc., San Jose, focusing on the development of micro-drives for portable information storage applications. While at Stanford, he worked with Dr. Kenny at Stanford Microstructures and Sensors Laboratory and focused his PhD work on high-performance tunneling MEMS sensors. He currently oversees graduate students in the Micro-Systems and Control Laboratory, whose research activities cover a variety of areas such as biomimetic array chip for bio-object manipulation targeting for tissue engineering/drug screening applications, micro-fluidic integration chips for bio-medical and micro-fuel cell applications, protein chip, tunable photonic crystal for telecommunication applications, advanced tunable MEMS grating and microsystem robust control.